



# The issues and tentative solutions for contrast-enhanced magnetic resonance imaging at ultra-high field strength

Peter Fries,<sup>1,\*</sup> John N. Morelli,<sup>2</sup> Francois Lux,<sup>3</sup> Olivier Tillement,<sup>3</sup> Günther Schneider<sup>1</sup> and Arno Buecker<sup>1</sup>

Magnetic resonance imaging (MRI) performed at ultra-high field strengths beyond 3 Tesla (T) has become increasingly prevalent in research and preclinical applications. As such, the inevitable clinical implementation of such systems lies on the horizon. The major benefit of ultra-high field MRI is the markedly increased signal-to-noise ratios achievable, enabling acquisition of MR images with simultaneously greater spatial and temporal resolution. However, at field strengths higher than 3 T, the efficacy of Gd(III)-based contrast agents is diminished due to decreased  $r_1$  relaxivity, somewhat limiting imaging of the vasculature and contrast-enhanced imaging of tumors. There have been extensive efforts to design new contrast agents with high  $r_1$  relaxivities based on macromolecular compounds or nanoparticles; however, the efficacy of these agents at ultra-high field strengths has not yet been proven. The aim of this review article is to provide an overview of the basic principles of MR contrast enhancement processes and to highlight the main factors influencing relaxivity. In addition, challenges and opportunities for contrast-enhanced MRI at ultra-high field strengths will be explored. Various approaches for the development of effective contrast agent molecules that are suitable for a broad spectrum of applied field strengths will be discussed in the context of the current literature. © 2014 Wiley Periodicals, Inc.

## How to cite this article:

*WIREs Nanomed Nanobiotechnol* 2014. doi: 10.1002/wnan.1291

## INTRODUCTION

With the advent of magnetic resonance imaging (MRI) and its introduction into clinical medicine in the early 1980s, it was expected that MR imaging would be reserved for evaluation of the musculoskeletal system and the central nervous system. Due to long acquisition times, imaging of other

structures was markedly limited secondary to artifacts from patient respiratory motion, cardiac pulsation, and/or bowel peristalsis. As a consequence, MR imaging of the heart, great vessels, abdominal organs, and bowel was considered impossible. At that time, most MR systems operated at field strengths between 0.1 and 0.5 Tesla (T). However with further technical evolution, MRI scanners operating at field strengths between 1.5 and 3 T have become the clinical standard. At present MRI is utilized clinically for imaging of essentially all anatomical regions including the abdomen and heart due to the high temporal and spatial resolutions obtainable.<sup>1</sup>

The underlying factor driving these advances is the linear relationship between the signal available from mobile protons and the field strength of the main

\*Correspondence to: drpeterfries@googlemail.com

<sup>1</sup>Clinic of Diagnostic and Interventional Radiology (Geb. 50.1), Saarland University Medical Center, Homburg, Germany

<sup>2</sup>Russell H Morgan Department of Radiology & Radiological Science, Johns Hopkins University, Baltimore, MD, USA

<sup>3</sup>Institut Lumière Matière, Université Claude Bernard Lyon 1, Lyon, France

Conflict of interest: The authors have declared no conflicts of interest for this article.

magnetic field ( $B_0$ ). With increasing field strength, an increasing number of spins with higher energy levels in the parallel and antiparallel orientations contribute to the obtainable signal. This improved level of image signal in relation to image noise, known as the signal-to-noise ratio (SNR), may be used either to acquire images with increased spatial resolution, to expedite the sequence acquisition, or some combination thereof.<sup>2</sup>

The highest field strength utilized in the clinical routine today is 3 T. Apart from these clinical scanners, MR systems operating between 4.7 and 17 T are used for preclinical small animal experimental studies. Recently, human whole body scanners with field strengths beyond 7 T have been installed, but these are still utilized primarily for experimental, preclinical purposes.<sup>3</sup>

The benefits of the high temporospatial resolution obtainable at ultra-high field strengths are not without disadvantages. These include a higher specific absorption rate (SAR), reflecting a greater degree of energy deposition to the examined organism, as well as a greater propensity for certain types of artifacts. In particular, artifacts related to differences in tissue susceptibility, inhomogeneous radiofrequency penetration, and magnetic field inhomogeneity may degrade image quality based on, respectively, signal alteration, image distortion, and dielectric artifacts.<sup>2</sup> For human imaging beyond 3 T, there are additional limitations including a significantly higher rate of vertigo and other side effects.<sup>4</sup>

There are several additional challenges to imaging at ultra-high field strengths such as alterations in image contrast based on field strength dependent changes in tissue relaxation times (i.e., T1 and T2). Moreover, properties of available contrast agents are altered at ultra-high field strengths: longitudinal relaxivity ( $r_1$ ) decreases and T2\* effects become more dominant. These effects can degrade image quality and potentially reduce diagnostic accuracy. In recent years, the design of contrast agents with high  $r_1$  relaxivities has become a major research topic. In particular, gadolinium chelates with protein interactions have proven effective at field strengths up to 3 T. However, these agents may be less efficacious at ultra-high field strengths such as 7 T. Macromolecular contrast agents and nanoparticles represent promising contrast agents for ultra-high field applications.

The aim of this review article is to highlight basic principles of MR contrast enhancement processes, to discuss challenges with contrast-enhanced imaging at ultra-high field strengths, and to propose potential solutions.

## FACTORS INFLUENCING MR SIGNAL IN CONTRAST-ENHANCED IMAGING

Currently, approximately one third of all clinical MRI studies include administration of an intravenous contrast agent.<sup>5,6</sup> A total of 10 million contrast-enhanced MRI scans per year are performed worldwide.<sup>7</sup> The majority of contrast agents used in this setting are non-specific gadolinium (Gd)-based chelates with an extracellular distribution and T1 relaxation properties.<sup>5</sup> Improved image contrast is achieved as these compounds accumulate in certain tissues, decreasing T1 relaxation times relative to the surrounding background. On T1-weighted images, there is thus an increase in the signal intensity of such tissues compared to background. However, contrast enhancement is a complex process and the MR signal of a T1-weighted pulse sequence depends on many factors such as the strength of the applied magnetic field, as well as sequence parameters such as repetition time (TR), time to echo (TE), and flip angle (FA). The quantity of contrast agent within the tissue of interest and properties such as  $r_1$  and  $r_2$  relaxivity are also important considerations.

### Contrast Agent Relaxivities $r_1$ and $r_2$

Contrast agents are characterized by their relaxivities  $r_1$  and  $r_2$ . These are defined by the change in water proton relaxation rates  $R_1$  ( $=1/T_1$ ) and  $R_2$  ( $=1/T_2$ ) in the presence of a certain concentration of administered contrast agent [CA]<sup>8</sup>:

$$r_1 = \frac{\Delta(1/T_1)}{[CA]} = \frac{\Delta R_1}{[CA]} \quad (1)$$

$$r_2 = \frac{\Delta(1/T_2)}{[CA]} = \frac{\Delta R_2}{[CA]} \quad (2)$$

In general, MRI contrast agents may be divided in two broad categories—T1 and T2 agents. For a given concentration, T1 agents typically alter the  $1/T_1$  of a tissue more than  $1/T_2$  due to a fast transverse relaxation. Thus, tissues accumulating Gd(III)-based T1 agents demonstrate a reduction of their T1 relaxation times compared to background.<sup>9</sup> Due to the signal enhancement of the Gd(III) accumulating tissues, these agents are also referred to as positive contrast agents. However, depending on the contrast agent dose and the pulse sequence applied [such as dynamic susceptibility enhancement (DSE)], Gd(III)-based agents may also serve as T2\* agents. T2 agents induce a predominant increase of  $1/T_2$  resulting in a decrease of signal intensity. As a consequence,

these agents are referred to as negative contrast agents. Superparamagnetic iron oxide particles (SPIOs) or ultra-small superparamagnetic iron oxides (USPIOs) are examples of such T2\* agents.<sup>7</sup> Yet, USPIO also provide sufficient r1 relaxivity to be utilized as a T1 agent for dynamic contrast-enhanced (DCE) MRI studies of the liver (obtained acquiring T1-weighted gradient echo sequences). Because positive contrast agents are the agents overwhelming utilized in the clinical routine, they remain the focus of the subsequent discussion in this manuscript.

Relaxivities of contrast agents are not constant but depend upon several external factors such as temperature and the applied field strength as well as some intrinsic factors such as the structure of the Gd(III)-complex. In particular, the latter has tremendous influence on rotational dynamics of the molecule and subsequently the process of spin-lattice relaxation. In addition, the accessibility of water molecules to the Gd(III)-ion, the ion to water distance, and the time constants governing the exchange rate of relaxed water in the first and second coordination sphere with bulk water in the periphery play important roles in this process.<sup>7,8</sup> Simplified, these factors describe the interaction of Gd(III) with water molecules over time. At higher field strengths, these complex interactions are altered to different degrees limiting the physical relaxation process. For Gd-based agents, the most frequently used compounds in clinical MRI, r1 relaxivities typically decrease with increasing field strength and r2 effects become more prominent. This effect is more pronounced for larger Gd-complexes or complexes bound to albumin (i.e., MS-325) while low-molecular weight compounds like Gd-DTPA or Gd-DOTA are less prone to this phenomenon.<sup>7,10,11</sup>

### Enhancement Process

The process of contrast enhancement is based on a complex physicochemical dipolar interaction between water protons with a Gd(III) ion which, in most instances, is located in the center of a chelate molecule (Figure 1).<sup>11–16</sup> In theory, the contrast agent molecule and the water protons interact on different levels depending on the proximity to the Gd(III)-core with a  $1/r^6$  dependence (where  $r$  is the distance between the water and the lanthanide ion). This can be described as a model of different solvation spheres.<sup>7,8</sup> Herein, the inner sphere is characterized by a direct coordination of water oxygen to the Gd(III) where the water molecule and Gd-ion are in closest proximity. In the second coordination sphere, water molecules hydrate the complex with a shorter residence time than in the inner sphere, but with a longer residence time than the average translational diffusion time of surrounding

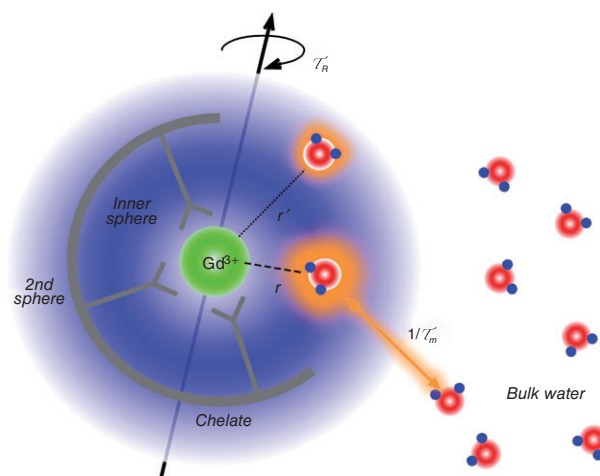


**FIGURE 1** | The variables influencing the physicochemical process of enhancement for a Gd(III)-based contrast agent. Here,  $r$  and  $r'$  represent the distance between the Gd(III)-ion and the water molecules in the inner and second hydration spheres, respectively.  $\tau_R$  represents the rotational correlation time of the contrast agent complex, reflecting the tumbling rate.  $1/\tau_m$  reflects the water exchange rate between the inner sphere and the surrounding bulk water with  $\tau_m$  corresponding to the mean residence time of the water molecule in the inner sphere.

solvent water. The distance of these water molecules from the Gd(III) is greater than for the inner sphere. Both, the inner and second sphere water molecules exchange with surrounding bulk water molecules at different rates. The outer sphere is less organized, and the interaction of water molecules with Gd(III) is solely determined by translational diffusion and the distance of the closest approach of water to Gd(III).

The entire relaxation process can be considered as summation of all water proton interactions with the Gd(III)-ion in all three different spheres. However, the main contribution is derived from the inner and second sphere while the contribution from the outer sphere water molecules is negligible. The T1 relaxation itself is based on a dipolar process depending on the number of water molecules involved, their rate of exchange with surrounding solvent water, their proximity to the Gd-center, and the correlation time ( $\tau_c$ ).<sup>7</sup> Correlation time is a constant characterizing fluctuating magnetic dipoles that can induce spin relaxation and spin transition. These fluctuating magnetic fields may be induced by several factors, such as the electronic relaxation at the Gd(III) ion, rotational diffusion of the contrast agent complex, and water exchange with the inner and second coordination sphere.

### Inner Sphere Relaxivity

Inner sphere relaxivity [ $r_1$ (IS)] depends on the hydration number ( $q$ ) of the contrast agent complex, the

water concentration  $[H_2O]$ , the T1 relaxation time of water hydrogen in the inner sphere ( $T_{1m}$ ), and the water residency time in the inner sphere ( $\tau_m$ ). Based on this consideration, relaxivity can theoretically be improved by increasing the hydration number or by decreasing  $T_{1m}$  and the water residency time  $\tau_m$ .

### Water Exchange Rate

Water exchange between the different categories of spheres around Gd(III) and the surrounding bulk water plays an important role in relaxivity. The faster the coordinated water can exchange with the surrounding bulk water, the more efficient the relaxation effects can be transferred to the surrounding bulk solvent. However, such water exchange must also be sufficiently slow. In other words, the water residency time at the inner sphere must be long enough to enable inner sphere water to coordinate to Gd(III) and to achieve sufficient relaxation. On the other hand, if the water exchange is too slow, then the relaxation effect cannot be transferred effectively to the surrounding water solvent.

### Hydration Number

The hydration number ( $q$ ) indicates the number of water molecules coordinated to the Gd(III) ion within the inner sphere of the contrast agent complex.  $r_1$  relaxivity is linearly proportional to the hydration number ( $q$ ) of the contrast agent complex. However, Gd(III) complexes with higher hydration numbers may demonstrate decreased thermodynamic stability and also allow other molecules to bind to the complex. This can result in significant toxicity issues due to the release of Gd(III), which is a toxic metal ion, an issue discussed in more detail below.

### Rotational Correlation Time

The rotational correlation time is a parameter describing the time dependence of the tumbling of a given molecule. Specifically, it is defined as the time constant for an exponential decay of an autocorrelation function of rotational motion. It roughly reflects the average time a molecule needs to rotate one radian. Usually, small molecules demonstrate a short rotational correlation time while larger molecules exhibit longer rotational correlation times. Contrast agent complexes with increased rotational correlation times usually demonstrate an improved interaction with the water protons and thus higher relaxation rates.<sup>17</sup> Thus, one possible way to design more potent contrast agents is by constructing larger molecules by binding paramagnetic complexes to nanostructures or to compounds with transient interactions with larger molecules such as plasma proteins. In the latter, the relaxation of water protons will be influenced

by a combination of the rotational correlation times of both the plasma protein and the contrast agent molecule itself.

## THE EFFECTS OF INCREASING FIELD STRENGTH ON GD-BASED CONTRAST AGENTS

### Change of Relaxivities and Relaxation Times

For high field and ultra-high field imaging, the most important problem in contrast-enhanced MRI is the decrease of  $r_1$  and  $r_2$  relaxivities with increasing field strength. This predominantly affects the  $r_1$  relaxivity of Gd(III)-based contrast agents (Figure 2) and is less pronounced for  $r_2$  relaxivities.<sup>8,10,18,19</sup> As a consequence, the positive enhancement properties of a T1 agent will be diminished, and the negative influences of the T2 and T2\* effects, which result in a loss of signal, become more prominent. Therefore, the  $r_2/r_1$  relation is often considered an important parameter to assess the performance of a given contrast agent at different field strengths (Table 1). At the same time T1 relaxation times of tissues, in general, tend to increase with higher field strengths resulting in improved background suppression.<sup>20,21</sup> In theory, this may enable a reduction in the administered contrast agent dose required to obtain a given level of contrast enhancement at higher field strengths.

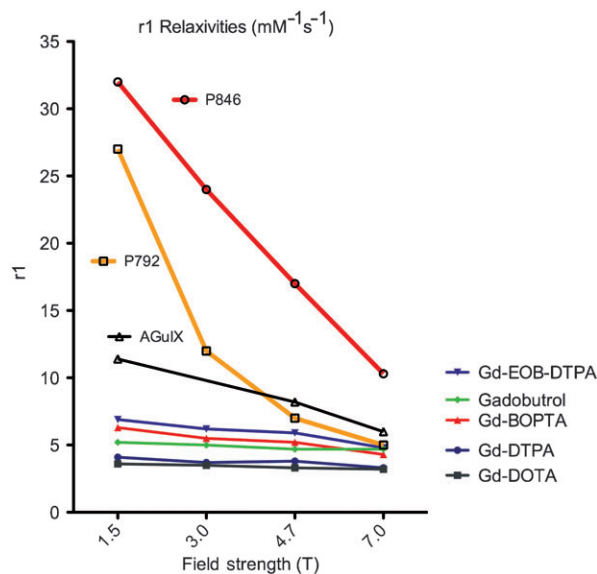


**FIGURE 2** | The field dependency of the  $r_1$  relaxivities for different clinical and experimental Gd(III)-based contrast agents. While  $r_1$  is fairly constant for the low-molecular compounds for a broad spectrum of field strengths, macromolecular agents demonstrate a large decrease in  $r_1$  at higher field strengths.

**TABLE 1** | r1 and r2 Relaxivities (values in mM<sup>-1</sup> s<sup>-1</sup>) of Different Gd(III)-based Contrast Agents at Different Field Strengths (37°C, in HSA 4%)<sup>31,33,38</sup>

		1.5 T	3.0 T	4.7 T	7.0 T
Gd-DOTA	r1	3.5	3.4	3.3	3.0
	r2	4.2	4.2	4.2	4.0
	r2/r1	1.2	1.2	1.2	1.3
P846	r1	32	24	17	10.3
	r2	41	34	23	37
	r2/r1	1.28	1.41	1.4	3.6
P792	r1	27	12	7	5
	r2	68	68	66	42
	r2/r1	2.52	5.67	9.43	8.4

### Influence of Magnetization

One possible explanation for the increase of T2 and T2\* effects of Gd(III) compounds at higher field strengths lies in an increased magnetization of paramagnetic complexes. While superparamagnetic iron oxides usually reach full magnetization at a field strength of approximately 0.5–1 T, Gd(III) complexes still demonstrate an increasing magnetization with increasing field strengths beyond 1 T.<sup>22</sup> As a consequence, susceptibility effects of such compounds are more pronounced at higher field strengths leading to a more dominant T2 and T2\* effect. In particular, this effect is notable in areas with high contrast agent concentrations, such as the contrast agent bolus arrival after intravenous injection. As a result, increasing contrast agent doses at high field strengths to compensate for the decreased r1 relaxivities will not necessarily be effective.<sup>8</sup>

## MECHANISMS FOR INCREASING MR SIGNAL IN CONTRAST-ENHANCED IMAGING AT ULTRA-HIGH FIELD STRENGTHS

### Increasing the Contrast Agent Dose

At first glance, increasing the contrast agent dose is the most intuitive way to increase the extent of enhancement on an MR imaging study. This approach can in part compensate for the decrease in r1 of a given Gd(III)-based contrast agent at higher field strengths. However, administering higher contrast agent doses also has some disadvantages.

First, the increase of contrast enhancement with increasing doses is not linear, but rather shows a plateau of maximum inducible signal.<sup>23</sup> Thereafter, the MR signal starts to decline with further increases

in the administered contrast agent dose. This is primarily based on the previously described phenomenon whereby T2\* effects become more prominent at increasing field strengths and interfere with positive signal enhancement based on T1 shortening. The increasing T2\* effects can be explained by an increasing magnetization of Gd(III) as described previously in this article. This detrimental interference of T2\* effects may even overcome the positive effects of prolonged background tissue T1 relaxation times at higher field strengths.

Another important dilemma in administering higher doses of contrast agent is the clinical concern for nephrogenic systemic fibrosis (NSF). It has been shown that the occurrence of NSF in patients with impaired renal function not only depends on the stability of the Gd-complex but also correlates with the number of total contrast agent administrations as well as the dose of the Gd-based contrast agent.<sup>24–27</sup> Therefore, high dose contrast agent administration in ultra-high field MRI may not be a safe way to achieve sufficient enhancement, particularly in patients with chronic kidney disease.

### Increasing r1

Increasing the r1 relaxivity of a given contrast agent would result in greater enhancement for a given concentration of gadolinium chelate. Extensive past efforts have been devoted to the design of novel contrast agents with increased r1 relaxivities. Some possible approaches to achieve this goal are described subsequently.

### Increasing the Rotational Correlation Time

As described previously, the interaction of water protons and the Gd(III) core with subsequent relaxation of the water protons and exchange with surrounding bulk water are critical factors in an efficient enhancement process. The interaction of the contrast agent complex with solvent water can be markedly improved if the rotational correlation time of the complex is increased.<sup>17,28</sup>

### Macromolecular Complexes

One way to leverage these aspects of contrast agent design is to increase the weight of the contrast agent complex. This can be achieved by adding larger side chains or molecular complexes to low-molecular Gd-chelates such as Gd-DTPA or Gd-DOTA. Representative agents employing this approach are, among several others, the experimental compounds P846<sup>29–33</sup> and P792<sup>31,33–38</sup> (Figure 3).

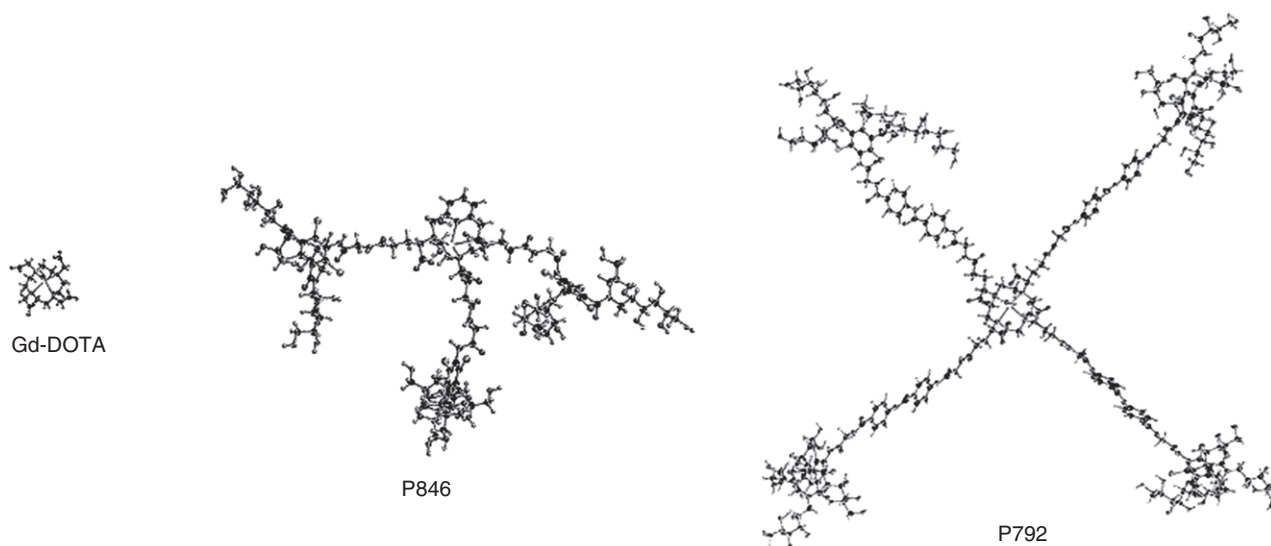


**FIGURE 3** | Molecular structures of three Gd(III)-based contrast agents. Gd-DOTA represents a low-molecular chelate with an extracellular distribution. In the case of P846 and P792, three and four side arms are added, respectively, thus resulting in a greater molecular mass and a larger hydrodynamic diameter. (Reprinted with permission from Ref.<sup>31</sup> Copyright 2009 Lippincott Williams & Wilkins, Inc.)

P846 is an intermediate-sized, macrocyclic three-armed chelate with one Gd(III)-ion at the center of the complex. With a molecular mass of 3.5 kDa, it has almost six times the mass of Gd-DOTA (0.6 kDa). With a hydrodynamic diameter of approximately 4 nm, it is substantially larger than Gd-DOTA (approximately 1 nm). As a result, P846 demonstrates markedly higher  $r_1$  relaxivities at different field strengths as compared to the conventional low-molecular complex Gd-DOTA (see Table 1).

P792 (Gadomelitol/Vistarem) consists of a monomeric macromolecular organic Gd-chelate with a DOTA species in the center of the complex linked to hydrophilic bulky groups in the periphery. With a molecular mass of approximately 6.5 kDa, it is about 10 times larger than Gd-DOTA and has a hydrodynamic diameter of around 7 nm. Again, this leads to a marked improvement of  $r_1$  relaxivity at both clinical field strengths between 1.5 and 3 T and ultra-high field strengths such as 4.7 or 7 T.

Table 1 also displays the *in vitro*  $r_2$  relaxivities and the  $r_2/r_1$  relationships of these compounds, which increase particularly quickly for the macromolecular compounds at higher field strengths. In distinction, the  $r_2/r_1$  of the low-molecular agent Gd-DOTA is fairly constant for all applied field strengths.

In a rat brain glioma study performed at 3 T, two macromolecular contrast agents, P846 and P792, were compared with the clinically approved low-molecular contrast agent Gd-DOTA.<sup>31</sup> A standard clinical dose of Gd-DOTA (0.1 mmol/kg body weight) was administered. For the macromolecular compounds, the

contrast agent doses were reduced—to 0.025 mmol/kg body weight for P846 and 0.05 mmol/kg body weight for P792—in order to compensate for the differences in  $r_1$  relaxivities. All three agents were randomly administered to each rat with 48 h between doses to allow sufficient clearance of each contrast agent from the body. T1-weighted gradient echo sequences were performed at consecutive time points. SNR, CNR, and lesion enhancement were measured to determine the evolution of contrast enhancement (see Figure 4). Interestingly, P846 demonstrated comparable tumor enhancement relative to Gd-DOTA at only one fourth of the administered dose. In distinction, tumor enhancement after administration of P792 was significantly lower versus Gd-DOTA and P846 (Figure 4(b)). This is attributable to the large molecular mass and hydrodynamic size of P792, which limits P792's passage across the damaged blood-brain-barrier. As a consequence, P792 is considered a compound with an intravascular rather than extracellular distribution. While P792 thus may be useful for cardiovascular imaging, it is less suitable for imaging applications that rely on enhanced permeability and retention (EPR) principles. In distinction, P846 exhibits markedly improved lesion enhancement indicating that there is significant extravasation of the compound from the vasculature and subsequent accumulation in tumors. Thus, compounds with moderately increased molecular weight and size, such as P846, may represent the optimal combination of a high  $r_1$  relaxivity with retention of enhancement properties analogous to clinically

approved low-molecular agents with extracellular distributions. However as indicated in Figure 2, when moving beyond 3 T, P846 also exhibits a marked drop of  $r_1$  relaxivity *in vitro* which could mitigate the improved enhancement properties at ultra-high field strengths. This principle is supported by recent data comparing P846 with Gd-DTPA in a rat model of hepatic colorectal cancer metastases performed at 9.4 T.<sup>39</sup> In this intra-individual comparison, both agents were administered at a dose of 0.1 mmol/kg body weight. Although P846 demonstrated significantly greater lesion enhancement, the dose utilized in that experiment was four times greater than in the previously described 3 T study. Thus, successful administration of P846 at field strengths beyond 7 T may require standard clinical doses of 0.1 mmol/kg body weight.

### Plasma Protein Interaction

The introduction of covalent or noncovalent binding with plasma proteins (i.e., albumin)<sup>40</sup> can also increase the rotational correlation times of contrast agents. Examples of clinically approved contrast agents that employ this technique include Gd-BOPTA (MultiHance<sup>®</sup>, Bracco Imaging SpA, Milan, Italy), Gd-EOB-DTPA (Primovist<sup>®</sup>, Bayer Healthcare, Berlin, Germany), and MS-325 (Vasovist<sup>®</sup>, Bayer Healthcare).<sup>28</sup> However, linking Gd-complexes to larger molecules such as plasma proteins does not mean that the rotational correlation time of the compound is equal to that of the plasma protein. Rather, it is an average of the rotational correlation times of both molecules. Contrast agents exhibiting covalent or noncovalent bonds to plasma proteins demonstrate a markedly increased  $r_1$  for field strengths between 0.5 and 1 T; however,  $r_1$  relaxivities for these compounds drop when moving to higher field strengths. In this setting, rotational correlation might be slowed beyond the Larmor frequency at ultra-high field strengths, thus impairing an efficient relaxation process.<sup>7</sup>

Depending on the degree of plasma protein binding, the aforementioned agents demonstrate increased intravascular retention and may thus be considered blood-pool contrast agents. One such example is MS-325, which binds strongly but reversibly to human serum albumin (up to 96.2% binding at a dose of 0.1 mmol/L). In addition to their use in MR angiography, such agents may be useful in monitoring tumor response after anti-vascular drug therapy.<sup>28,41</sup>

### Nanoparticles

In recent years, the development and application of nanoparticles in biomedicine has become increasingly important. So-called 'theragnostics' combine multiple

features. They may serve as contrast agents for different imaging modalities like MRI, computed tomography, scintigraphy, or optical imaging while simultaneously enabling therapeutic options such as hypothermia induction, drug delivery, neutron therapy, or radiosensitization.<sup>42–44</sup>

In terms of contrast-enhanced MRI, nanoparticle compounds not only have a relatively large molecular size but also possess the ability to bind several Gd(III) complexes at a time. This leads to improved enhancement properties of the compound.<sup>45,46</sup>

However, construction of multifunctional nanoparticles often requires linking of particular side chains and large molecule species to the core complex. This can result in an inappropriate increase in molecular size or weight with a subsequent, undesirable accumulation of the nanoparticle in the body. In most instances, the macrophages of the reticulo-endothelial system (RES) will take up such nanoparticles. In particular, particles with molecular sizes larger than 50 nm are prone to accumulate in the RES of the lung and the liver.<sup>47</sup> As a consequence, it remains challenging to combine biocompatibility and multi-functionality while avoiding undesirable nanoparticle accumulation. For instance, nanoparticles based on quantum dots or gold clusters require particular coatings to ensure biocompatibility and frequently lead to an undesirably high molecular mass.<sup>48,49</sup>

In addition, nanoparticles, once administered, should efficiently be removed from the organism. In most cases, this occurs via renal excretion. However, sufficiently prompt renal clearance is only achievable for particles with hydrodynamic diameters smaller than 5.5 nm.<sup>50</sup> For larger sizes between 5 and 10 nm, the elimination route depends upon the molecule surface.<sup>51</sup> Recently, optimization of chemical processes has enabled synthesis of nanoparticles with multimodal features and molecular sizes between 3 and 7 nm.<sup>45,52</sup> For instance, AGuIX<sup>®</sup> is an ultra-small nanoparticle based on a polysiloxane core linked to 10 DOTA ligands in the periphery (Figure 5). These DOTA complexes can chelate different ions, i.e., Gd(III) or <sup>111</sup>I. Thus, AGuIX can serve as a multimodal contrast agent for MRI, CT, optical imaging, or scintigraphy.<sup>45,53</sup> With a hydrodynamic size of approximately 3 nm and a molecular mass of 8.5 kDa, this particle has been shown to be sufficiently small to enable rapid renal excretion and to avoid accumulation within RES macrophages in experimental studies.<sup>45,54</sup> Due to the increased molecular size and the rigidity of the inorganic matrix, AGuIX exhibits a two fold increase of  $r_1$  ( $6.0 \text{ mM}^{-1} \text{ s}^{-1}$ ) at 7 T per Gd(III) as compared to Gd-DOTA ( $3.0 \text{ mM}^{-1} \text{ s}^{-1}$ ). In

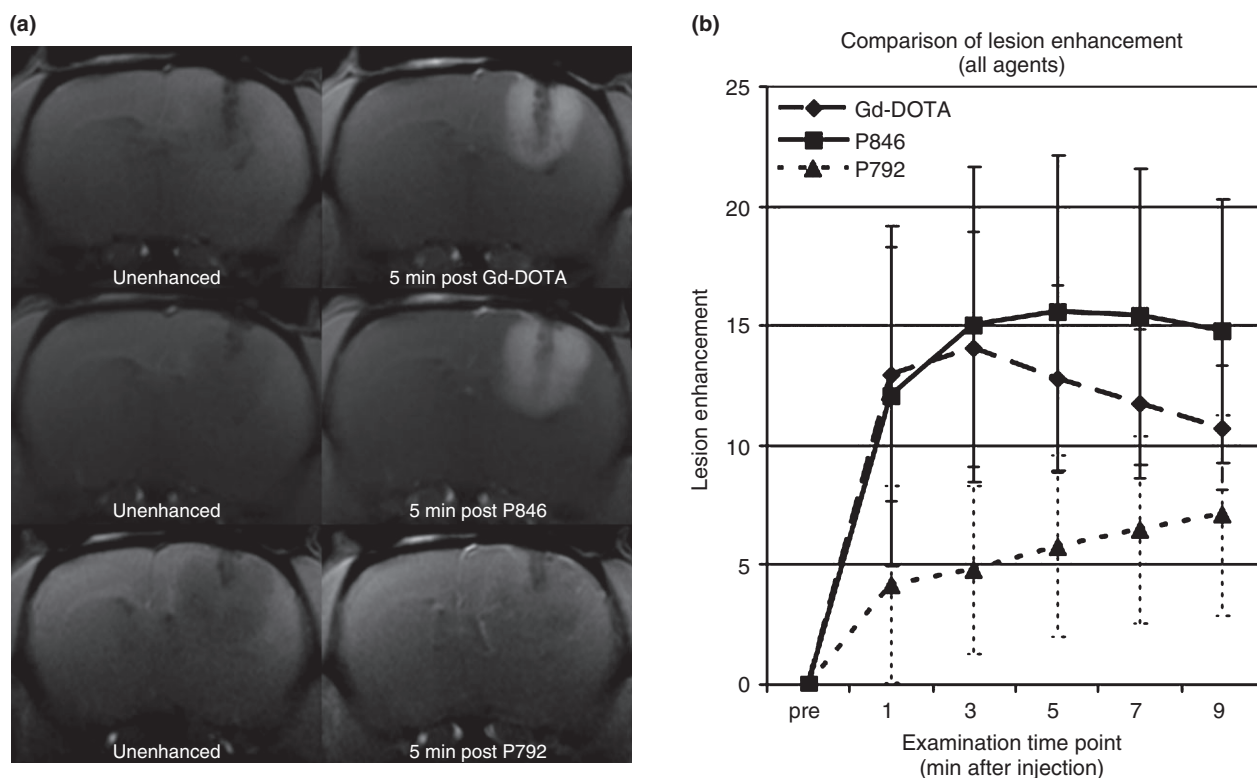


**FIGURE 4** | Coronal T1-weighted sequences acquired at the level of an experimental brain glioma in a rat study with the unenhanced scans displayed on the left side and the corresponding contrast-enhanced scans on the right. Intra-individual administration of three different Gd(III)-based contrast agents was performed (Gd-DOTA, P846, P792) with the contrast agent doses being adjusted to compensate for the different relaxivities. P846 (@0.025 mmol/kg body weight) shows comparable enhancement relative to Gd-DOTA (@0.1 mmol/kg body weight). In distinction, P792 (@0.05 mmol/kg body weight) demonstrates considerably less enhancement, which can be explained by the larger molecular size of the compound and a smaller amount of extravascular extravasation. (Reprinted with permission from Ref.<sup>31</sup> Copyright 2009 Lippincott Williams & Wilkins, Inc.)

addition to its contrast agent abilities, AGuIX demonstrates radio-sensitizing effects *in vitro* and *in vivo* and thus may be beneficial for MRI-guided cancer radiotherapy.<sup>55,56</sup>

A recent study has demonstrated the beneficial contrast enhancement properties of AGuIX at 9.4 T.<sup>57</sup> In this intra-individual comparison trial in a rat model of hepatic colorectal cancer, AGuIX was administered at a dose of 0.01 mmol/kg body weight and compared with Gd-DOTA at a 0.1 mmol/kg body weight dose. In this way, equivalent Gadolinium doses were given, as AGuIX consists of a cluster of 10 Gd-DOTA molecules linked to a nanoparticle. The acquired contrast-to-noise ratio between normal liver tissue and the liver tumors was statistically significantly greater for AGuIX compared to Gd-DOTA. Similar kinetics were observed between the molecules, both of which demonstrated strong peak enhancement immediately after administration followed by continuous washout during the remainder of the examination (Figure 6). Thus, based on its rather small size and hydrodynamic diameter, AGuIX may serve as an

effective extracellular contrast agent for ultra-high field strength applications.

### Dendrimer-Based Gd(III) Agents

Dendrimers typically consist of repeatedly branched molecules symmetrically arranged around a core resulting in a spherical three-dimensional structure. Polypropyleneimine diaminobutane (DAB) and polyamidoamine (PAMAM) are two representative examples of dendrimers.<sup>28</sup> Typical features of dendrimers include water solubility and the large number of coupling sites to other species such as chelating agents. Thus, DTPA or DOTA may bind covalently to the surface of dendrimers and host numerous Gd(III) ions. Depending on the size of the molecules or the groups functionalized to the complexes, dendrimers demonstrate different excretion rates and pathways of metabolism. While smaller sized dendrimers show high rates of renal excretion, larger sized dendrimers demonstrate a longer intravascular retention and may thus be used as blood-pool agents.<sup>58</sup> By functionalizing other ligands such as monoclonal antibodies



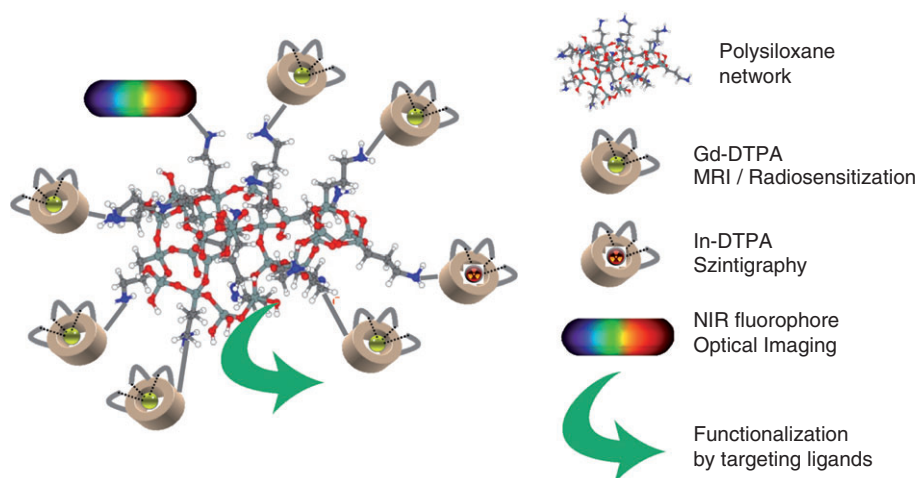


**FIGURE 5** | Schematic structure of AGuIX, which is based on a polysiloxane core and 10 DOTA species in the periphery that can bind to Gd(III) or  $^{111}\text{In}$ . In addition, NIR fluorophore or targeting ligands can be added enabling multimodal applications in diagnostic imaging and therapy.

or fluorophore, dendrimer-based complexes may be used as tumor specific or multimodal contrast agents in MRI and optical imaging.<sup>59,60</sup>

### Polymeric Gd(III) Complexes

Similar to dendrimer-based contrast agents, the improved enhancement properties of polymeric gadolinium complexes result from a large molecular mass, ranging from 15 kDa up to millions of Da, with subsequent reduction of the tumbling rate. In addition, these molecules may also bind several Gd(III) ions, improving relaxivity per molecule. Gadomer-17 is a representative of this class of contrast agents. The complex consists in a trimesoyl triamide core with 24 polyamines conjugated to chelators with the ability to bind 24 Gd(III) ions.<sup>61</sup> Due to its size of approximately 35 kDa, it is primarily restricted to the vascular compartment and subsequently may serve as a blood-pool contrast agent.<sup>62,63</sup> However, Gadomer-17 is still sufficiently small to be eliminated from the body in an unmetabolized form by glomerular filtration within 24 h.<sup>61</sup>

### Changing the Accessibility to and Number of the Water Protons with Access to the Gd-core

As stated previously increasing the hydration number of a Gd-complex is a mechanism by which  $r_1$  relaxivity can be increased. However, synthesis of Gd(III) co-ligands that allow for coordination of more than one water molecule to the inner sphere typically results in less stable compounds and less efficiency in terms of complexation of the Gd(III) ion. The decreased thermodynamic stability raises major

toxicity concerns. In addition, just as the complex is more open to coordination of water molecules, it is also prone to coordination of other competitive endogenous molecules such as phosphate or bicarbonate. Exchange of coordinated water with these endogenous molecules results in a drop of  $r_1$  relaxivity and, as a consequence, diminishes the beneficial effect of a higher hydration number.<sup>7,28</sup> However, recent studies have shown the feasibility of synthesis of contrast agent molecules with a high hydration number ( $q = 2$ ), sufficient Gd(III) complex stability, and resistance to detrimental anion coordination.<sup>64–66</sup>

As mentioned previously, Gd-H distance plays a major role in terms of  $r_1$  relaxivity as there is a  $1/r^6$  dependency. However, there are some caveats with respect to utilizing this factor to improve the relaxivity of a Gd(III) agent. In general, Gd-H ion-nucleus distances are difficult to assess. The distance can be measured by several methods: neutron diffraction on single crystals, isotopic exchange methods in very concentrated solutions, nuclear magnetic relaxation dispersion (NMRD), electron paramagnetic resonance (EPR), or by electron nuclear double resonance (ENDOR).<sup>7</sup> Recent studies have revealed that Gd-H distances for different commercially available Gd(III)-based contrast agents do not differ significantly ( $3.1 \pm 0.1 \text{ \AA}$ ).<sup>67,68</sup> Therefore, reduction of the Gd-H distance may not be a feasible option by which to optimize contrast agent enhancement properties.

### Properties of an Ideal Contrast Agent

In order to design a contrast agent with high  $r_1$  relaxivities for a broad spectrum of field strengths (i.e., between 1.5 and 9.4 T) some additional points should be taken into consideration.

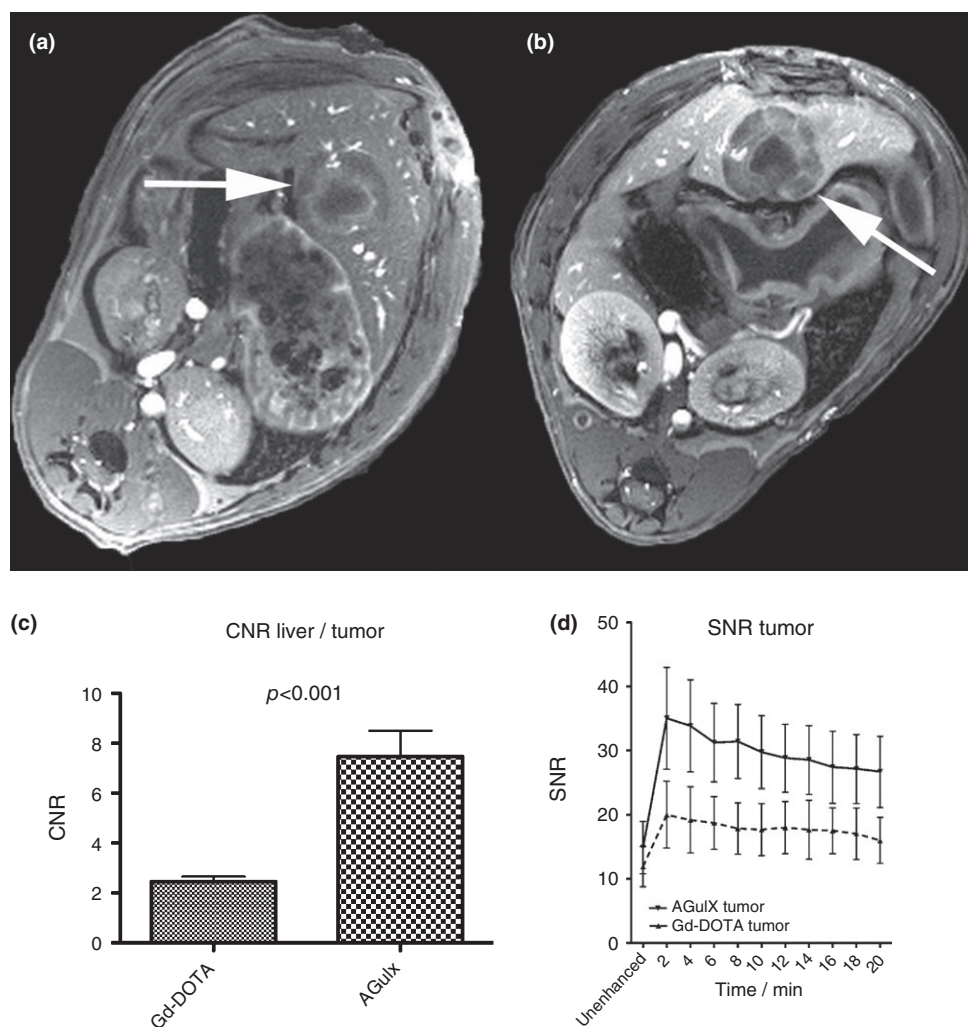


**FIGURE 6** | A T1-weighted axial image in a rat with a hepatic colorectal cancer metastasis (diameter approximately 8 mm, arrows) after administration of 0.1 mmol/kg body weight Gd-DOTA (a) and 0.01 mmol/kg body weight AGuIX (b). Although the doses of Gd are equivalent, post-contrast images with AGuIX better depict the mass relative to Gd-DOTA as is evident from the greater contrast-to-noise ratio (CNR, c) between normal liver tissue and the metastasis. Despite its greater molecular mass and size, AGuIX demonstrates enhancement kinetics comparable to a low-molecular contrast agent (d) with a strong, early peak enhancement followed by a continuous washout.

*In vitro* simulation data has demonstrated that the optimum correlation times for the spectrum of field strengths from 1.5 to 9.4 T lies between that of low-molecular weight agents with fast tumbling rates (i.e., Gd-DTPA or Gd-DOTA) and slow tumbling compounds with protein- or polymer-binding (i.e., MS-325). In particular, correlation times between 0.5 and 1.5 nanoseconds are considered efficient.<sup>8</sup> One possibility to achieve these intermediate correlation times is to create molecules with the Gd(III)-chelate placed in the barycenter of the molecule. As a consequence, the tumbling rate of the Gd(III)-chelate is close to that of the entire contrast agent molecule and less prone to effects of internal motion. This approach has been realized by creating glycoconjugated gadolinium

complexes<sup>69</sup> and also in the case of the aforementioned complex known as P792 (Vistarem).<sup>34</sup> Another approach is to link several Gd(III)-chelates together to a rigid polymer. In this case, the tumbling rates of the individual Gd(III)-chelates will be determined by the tumble rate of the large complex.<sup>70–73</sup>

There have been extensive research efforts into the design of contrast agents with high relaxivity across a broad spectrum of field strengths. However, high *in vivo* relaxivity does not directly translate into strong *in vivo* enhancement as was demonstrated in the aforementioned experiment comparing Gd-DOTA with P846 and P792. Larger macromolecular agents demonstrate slower and overall decreased accumulation in pathologic lesions such as brain tumors,

thus resulting in decreased enhancement relative to low-molecular weight or intermediate-sized contrast agents. In the previously described study, the greatest degree of enhancement in the brain glioma model was achieved with an intermediate-sized experimental compound, P846<sup>31</sup> (Figure 4). Since glioma enhancement requires extravasation into the extravascular space, enhancement with contrast agents based on larger molecules may be limited as the agents are predominantly restricted to the intravascular space. As a consequence, designing large contrast agent molecules in order to increase the  $r_1$  relaxivity may be counterproductive due to a reduced accumulation of the agents in pathologic lesions based on the EPR mechanism. However, utilization of these larger molecule agents may nevertheless prove useful in the context of MR imaging of the cardiovascular system.

## ALTERNATIVE APPROACHES TO CONTRAST-ENHANCED ULTRA-HIGH FIELD MRI

Despite efforts in ultra-high field MRI research, no major breakthroughs have been achieved with respect to clinical applications in humans for field strengths beyond 3 T. Still, there remain several ultra-high field imaging techniques that may become clinically relevant upon further development. Among these, one promising technique consists of MR spectroscopy and/or MR imaging of nuclei other than protons. The use of  $^{19}\text{F}$  as a substrate for MR imaging is a particularly interesting approach. Historically,  $^{19}\text{F}$  MRI is nearly as old as the first clinical applications of  $^1\text{H}$  MRI in the 1970s.<sup>74</sup> There are several important advantages of  $^{19}\text{F}$ . It is an isotope found naturally in the human body, as opposed to a toxic metallic ion like gadolinium. Further, the concentration of mobile  $^{19}\text{F}$  is relatively low, which results in limited background signal. Finally, its resonance frequency is similar to that of  $^1\text{H}$ .<sup>75</sup> Thus, a fluorine-based contrast agent could potentially provide very high contrast-to-noise ratios and specificity. However in  $^1\text{H}$  MRI, the fraction of nuclei contributing to the signal is near 60% of all nuclei present in the body. Due to the scarcity of mobile  $^{19}\text{F}$ , it remains very difficult to achieve sufficient signal. As a consequence fluorine-based contrast agents need to be highly concentrated within the tissue of interest and require a large load of  $^{19}\text{F}$  per molecule. One solution may be the use of perfluorocarbons (PFCs), which are organic molecules where numerous hydrogen atoms are replaced by  $^{19}\text{F}$ .<sup>75</sup>  $^{19}\text{F}$  MRI can potentially be useful in many applications including the visualization of inflammatory processes by tracking of immunocompetent cells,<sup>76</sup> *in vivo* visualization

of drug metabolism such as with 5-Fluorouracil,<sup>77</sup> assessment of pH and cations in tissues,<sup>78,79</sup> and MR imaging of the lung.<sup>80,81</sup> The fusion of  $^1\text{H}$  MR images, displaying tissue morphology, with  $^{19}\text{F}$  MR images enables exact localization of fluorinated substances, which are identified as 'hot spots' on the fused images.<sup>82</sup>

## CONCLUSION

For MR imaging between 1.5 and 3 T, several clinically approved MR contrast agents are useful in the workup of a broad spectrum of disease. With recent technical innovations, ultra-high field strength MRI scanners operating beyond 3 T have become increasingly common and are on the verge of clinical application. However, currently approved contrast agents are less efficient at ultra-high field strengths, demonstrating decreased  $r_1$  relaxivities. Increasing the contrast agent dose may only partially compensate for this negative effect as  $T_2^*$  effects also become more pronounced at ultra-high field strengths. Further, high doses of gadolinium chelate contrast agents are a poor option due to the risk of nephrogenic systemic fibrosis. Thus, additional progress must be made in the development of MR contrast agents that provide adequate contrast enhancement throughout a broad spectrum of field strengths and particularly at ultra-high field strengths. The ideal gadolinium based contrast molecule or nanoparticle for this purpose should demonstrate a high water exchange rate, a long water residence time, an intermediate tumbling rate, and a high hydration number. At the same time, for safety purposes, the ideal agent should also exhibit a high thermodynamic stability and a low kinetic dissociation rate. In addition, the ideal agent would be composed of a sufficiently small molecule to enable extracellular distribution and enhancement properties based on the EPR effect in addition to demonstrating rapid renal clearance and minimal reticulo-endothelial accumulation. Small nanoparticles that simultaneously bind several Gd(III)-chelates are promising agents for ultra-high field strength contrast-enhanced imaging. The addition of other species to these complexes may enable construction of multimodal agents as well as the development of therapeutic probes for drug delivery, heat induction, or radiosensitization.

Relative to MRI scanner technology, the development of contrast agents suitable for ultra-high field strength imaging suffers from additional regulatory restrictions. Since contrast agents are considered pharmaceuticals, applications in humans must comply with the same developmental guidelines established by local and national governments for standard

pharmaceutical drugs. Although such regulations are critical for ensuring maximum quality and safety, obtaining approval for such agents is currently a time-consuming, cost-intensive process. Consequently, contrast agent development currently lags behind the development of scanner technology. However, this fact should not discourage contrast media

research, but rather encourage development of more novel, innovative agents. Specifically, the combination of ultra-high field MR imaging systems with nanoparticle based multimodal probes could rapidly facilitate personalized diagnostic imaging, opening the door to new paradigms in disease diagnosis, treatment, and post-therapeutic monitoring.

## REFERENCES

1. Fries P, Runge VM, Kirchin MA, Watkins DM, Buecker A, Schneider G. Magnetic resonance imaging of the spine at 3 Tesla. *Semin Musculoskelet Radiol* 2008, 12:238–252.
2. Runge VM, Nitz WR, Schmeets SH, Schoenberg SO. *Clinical 3T Magnetic Resonance*. New York: Thieme; 2007.
3. Vaughan T, DelaBarre L, Snyder C, Tian J, Akgun C, Shrivastava D, Liu W, Olson C, Adriany G, Strupp J, et al. 9.4T human MRI: preliminary results. *Magn Reson Med* 2006, 56:1274–1282.
4. Theysohn JM, Maderwald S, Kraff O, Moeninghoff C, Ladd ME, Ladd SC. Subjective acceptance of 7 Tesla MRI for human imaging. *MAGMA* 2008, 21:63–72.
5. Aime S, Caravan P. Biodistribution of gadolinium-based contrast agents, including gadolinium deposition. *J Magn Reson Imaging* 2009, 30:1259–1267.
6. Caravan P, Ellison JJ, McMurry TJ, Lauffer RB. Gadolinium(III) chelates as MRI contrast agents: structure, dynamics, and applications. *Chem Rev* 1999, 99:2293–2352.
7. Caravan P. Strategies for increasing the sensitivity of gadolinium based MRI contrast agents. *Chem Soc Rev* 2006, 35:512–523.
8. Caravan P, Farrar CT, Frullano L, Uppal R. Influence of molecular parameters and increasing magnetic field strength on relaxivity of gadolinium- and manganese-based T1 contrast agents. *Contrast Media Mol Imaging* 2009, 4:89–100.
9. Zhou Z, Lu ZR. Gadolinium-based contrast agents for magnetic resonance cancer imaging. *WIREs Nanomed Nanobiotechnol* 2013, 5:1–18.
10. Rohrer M, Bauer H, Mintorovitch J, Requardt M, Weinmann HJ. Comparison of magnetic properties of MRI contrast media solutions at different magnetic field strengths. *Invest Radiol* 2005, 40:715–724.
11. Solomon I. Relaxation processes in a system of two spins. *Phys Rev* 1955, 99:559–565.
12. McConnell HM. Reaction rates by nuclear magnetic resonance. *J Chem Phys* 1958, 28:430–431.
13. Swift TJ, Connick RE. NMR-relaxation mechanism of O17 in aqueous solutions of paramagnetic cations and the lifetime of water molecules in the first coordination sphere. *J Chem Phys* 1962, 37:307–320.
14. Bloembergen N, Morgan LO. Proton relaxation times in paramagnetic solutions. Effects of electron spin relaxation. *J Chem Phys* 1961, 34:842–850.
15. Gueron M. Nuclear relaxation in macromolecules by paramagnetic irons: a novel mechanism. *J Magn Reson* 1975, 19:58–66.
16. Peters JA, Huskens J, Raber DJ. Lanthanide induced shifts and relaxation rate enhancement. *Prog Nucl Magn Reson* 1996, 28:283–350.
17. Borel A, Bean JF, Clarkson RB, Helm L, Moriggi L, Sherry AD, Woods M. Towards the rational design of MRI contrast agents: electron spin relaxation is largely unaffected by the coordination geometry of gadolinium(III)-DOTA-type complexes. *Chemistry* 2008, 14:2658–2667.
18. Pintaske J, Martirosian P, Graf H, Erb G, Lodemann KP, Claussen CD, Schick F. Relaxivity of Gadopentate Dimeglumine (Magnevist), Gadobutrol (Gadovist), and Gadobenate Dimeglumine (MultiHance) in human blood plasma at 0.2, 1.5, and 3 Tesla. *Invest Radiol* 2006, 41:213–221.
19. Noebauer-Huhmann IM, Szomolanyi P, Juras V, Kraff O, Ladd ME, Trattnig S. Gadolinium-based magnetic resonance contrast agents at 7 Tesla: in vitro T1 relaxivities in human blood plasma. *Invest Radiol* 2010, 45:554–558.
20. Rooney WD, Johnson G, Li X, Cohen ER, Kim SG, Ugurbil K, Springer CS Jr. Magnetic field and tissue dependencies of human brain longitudinal 1H2O relaxation in vivo. *Magn Reson Med* 2007, 57:308–318.
21. Pohmann R, Shajan G, Balla DZ. Contrast at high field: relaxation times, magnetization transfer and phase in the rat brain at 16.4T. *Magn Reson Med* 2011, 66:1572–1581.
22. Boxerman JL, Hamberg LM, Rosen BR, Weisskoff RM. MR contrast due to intravascular magnetic susceptibility perturbations. *Magn Reson Med* 1995, 34:555–566.
23. Hagberg GE, Scheffler K. Effect of r(1) and r(2) relaxivity of gadolinium-based contrast agents on the T(1)-weighted MR signal at increasing magnetic field strengths. *Contrast Media Mol Imaging* 2013, 8:456–465.

24. Perazella MA. Current status of gadolinium toxicity in patients with kidney disease. *Clin J Am Soc Nephrol* 2009, 4:461–469.
25. Thomsen HS, Morcos SK, Almen T, Bellin MF, Bertolotto M, Bongartz G, Clement O, Leander P, Heinz-Peer G, Reimer P, et al. Nephrogenic systemic fibrosis and gadolinium-based contrast media: updated ESUR Contrast Medium Safety Committee guidelines. *Eur Radiol* 2013, 23:307–318.
26. Thomsen HS. Nephrogenic systemic fibrosis: history and epidemiology. *Radiol Clin North Am* 2009, 47:827–831 vi.
27. Thomsen HS. How to avoid nephrogenic systemic fibrosis: current guidelines in Europe and the United States. *Radiol Clin North Am* 2009, 47:871–875 vii.
28. Rashid HU, Yu K, Zhou J. Lanthanide(III) chelates as MRI contrast agents: a brief description. *J Struct Chem* 2013, 54:223–249.
29. Jacquier A, Wendland M, Do L, Robert P, Corot C, Higgins CB, Saeed M. MR imaging assessment of the kinetics of P846, a new gadolinium-based MR contrast medium, in ischemically injured myocardium. *Contrast Media Mol Imaging* 2008, 3:112–119.
30. Peldschus K, Hamdorf M, Robert P, Port M, Graessner J, Adam G, Herborn CU. Contrast-enhanced magnetic resonance angiography: evaluation of the high relaxivity low diffusible gadolinium-based contrast agent P846 in comparison with gadoterate meglumine in rabbits at 1.5 Tesla and 3.0 Tesla. *Invest Radiol* 2008, 43:837–842.
31. Fries P, Runge VM, Bucker A, Schurholz H, Reith W, Robert P, Jackson C, Lanz T, Schneider G. Brain tumor enhancement in magnetic resonance imaging at 3 tesla: intraindividual comparison of two high relaxivity macromolecular contrast media with a standard extracellular gd-chelate in a rat brain tumor model. *Invest Radiol* 2009, 44:200–206.
32. Lemasson B, Serduc R, Maisin C, Bouchet A, Coquery N, Robert P, Le Duc G, Tropres I, Remy C, Barbier EL. Monitoring blood-brain barrier status in a rat model of glioma receiving therapy: dual injection of low-molecular-weight and macromolecular MR contrast media. *Radiology* 2012, 257:342–352.
33. Marty B, Djemai B, Robic C, Port M, Robert P, Valette J, Boumezbeur F, Le Bihan D, Lethimonnier F, Meriaux S. Hindered diffusion of MRI contrast agents in rat brain extracellular micro-environment assessed by acquisition of dynamic T1 and T2 maps. *Contrast Media Mol Imaging* 2013, 8:12–19.
34. Port M, Corot C, Raynal I, Idee JM, Dencausse A, Lancelot E, Meyer D, Bonnemain B, Lautrou J. Physicochemical and biological evaluation of P792, a rapid-clearance blood-pool agent for magnetic resonance imaging. *Invest Radiol* 2001, 36:445–454.
35. Gaillard S, Kubiak C, Stolz C, Bonnemain B, Chasard D. Safety and pharmacokinetics of p792, a new blood-pool agent: results of clinical testing in nonpatient volunteers. *Invest Radiol* 2002, 37:161–166.
36. Corot C, Violas X, Robert P, Gagneur G, Port M. Comparison of different types of blood pool agents (P792, MS325, USPIO) in a rabbit MR angiography-like protocol. *Invest Radiol* 2003, 38:311–319.
37. Corot C, Robert P, Lancelot E, Martinell A, Santus R. Distribution of gadomelitol in a human breast tumor model in mice. *MAGMA* 2005, 18:138–143.
38. Heilmann M, Vautier J, Robert P, Volk A. In vitro setup to study permeability characteristics of contrast agents by MRI. *Contrast Media Mol Imaging* 2009, 4: 66–72.
39. Fries P, Morr D, Müller A, Robert P, Dabew R, Massmann A, Seidel R, Bucker A, Schneider GK. Enhancement properties of a high relaxivity macromolecular Gd-based contrast agent (P846) compared with a standard extracellular Gd-chelate (Gd-DTPA) in rats with experimental liver tumours at 9.4 Tesla. *Insights Imaging* 2014, 5:S331.
40. Jacques V, Dumas S, Sun WC, Troughton JS, Greenfield MT, Caravan P. High-relaxivity magnetic resonance imaging contrast agents. Part 2. Optimization of inner- and second-sphere relaxivity. *Invest Radiol* 2010, 45:613–624.
41. Vogel-Claussen J, Gimi B, Artemov D, Bhujwalla ZM. Diffusion-weighted and macromolecular contrast enhanced MRI of tumor response to antivascular therapy with ZD6126. *Cancer Biol Ther* 2007, 6:1469–1475.
42. Petros RA, DeSimone JM. Strategies in the design of nanoparticles for therapeutic applications. *Nat Rev Drug Discov* 2010, 9:615–627.
43. Cuenca AG, Jiang H, Hochwald SN, Delano M, Cance WG, Grobmyer SR. Emerging implications of nanotechnology on cancer diagnostics and therapeutics. *Cancer* 2006, 107:459–466.
44. Kim J, Piao Y, Hyeon T. Multifunctional nanostructured materials for multimodal imaging, and simultaneous imaging and therapy. *Chem Soc Rev* 2009, 38:372–390.
45. Lux F, Mignot A, Mowat P, Louis C, Dufort S, Bernhard C, Denat F, Boschetti F, Brunet C, Antoine R, et al. Ultrasmall rigid particles as multimodal probes for medical applications. *Angew Chem Int Ed Engl* 2011, 50:12299–12303.
46. Ananta JS, Godin B, Sethi R, Moriggi L, Liu X, Serda RE, Krishnamurthy R, Muthupillai R, Bolskar RD, Helm L, et al. Geometrical confinement of gadolinium-based contrast agents in nanoporous particles enhances T1 contrast. *Nat Nanotechnol* 2010, 5:815–821.
47. Mignot A, Truillet C, Lux F, Sancey L, Louis C, Denat F, Boschetti F, Bocher L, Gloter A, Stephan O, et al. A top-down synthesis route to ultrasmall multifunctional Gd-based silica nanoparticles for theranostic applications. *Chemistry* 2013, 19:6122–6136.

48. Alric C, Taleb J, Le Duc G, Mandon C, Billotey C, Le Meur-Herland A, Brochard T, Vocanson F, Janier M, Perriat P, et al. Gadolinium chelate coated gold nanoparticles as contrast agents for both X-ray computed tomography and magnetic resonance imaging. *J Am Chem Soc* 2008, 130:5908–5915.
49. Cai W, Chen K, Li ZB, Gambhir SS, Chen X. Dual-function probe for PET and near-infrared fluorescence imaging of tumor vasculature. *J Nucl Med* 2007, 48:1862–1870.
50. Choi HS, Liu W, Misra P, Tanaka E, Zimmer JP, Ippy Ipe B, Bawendi MG, Frangioni JV. Renal clearance of quantum dots. *Nat Biotechnol* 2007, 25:1165–1170.
51. Faure AC, Dufort S, Josserand V, Perriat P, Coll JL, Roux S, Tillement O. Control of the in vivo biodistribution of hybrid nanoparticles with different poly(ethylene glycol) coatings. *Small* 2009, 5:2565–2575.
52. Benezra M, Penate-Medina O, Zanzonico PB, Schaefer D, Ow H, Burns A, DeStanchina E, Longo V, Herz E, Iyer S, et al. Multimodal silica nanoparticles are effective cancer-targeted probes in a model of human melanoma. *J Clin Invest* 2011, 121:2768–2780.
53. Bianchi A, Lux F, Tillement O, Cremillieux Y. Contrast enhanced lung MRI in mice using ultra-short echo time radial imaging and intratracheally administered Gd-DOTA-based nanoparticles. *Magn Reson Med* 2013, 70:1419–1426.
54. Miladi I, Duc GL, Kryza D, Berniard A, Mowat P, Roux S, Taleb J, Bonazza P, Perriat P, Lux F, et al. Biodistribution of ultra small gadolinium-based nanoparticles as theranostic agent: application to brain tumors. *J Biomater Appl* 2013, 28:385–394.
55. Mowat P, Mignot A, Rima W, Lux F, Tillement O, Roulin C, Dutreix M, Bechet D, Huger S, Humbert L, et al. In vitro radiosensitizing effects of ultrasmall gadolinium based particles on tumour cells. *J Nanosci Nanotechnol* 2011, 11:7833–7839.
56. Le Duc G, Miladi I, Alric C, Mowat P, Brauer-Krisch E, Bouchet A, Khalil E, Billotey C, Janier M, Lux F, et al. Toward an image-guided microbeam radiation therapy using gadolinium-based nanoparticles. *ACS Nano* 2011, 5:9566–9574.
57. Fries P, Morr D, Müller A, Lux F, Tillement O, Palm J, Schneider G, Seidel R, Buecker A. Evaluation of enhancement properties of gadolinium-labelled nanoparticles for contrast-enhanced MRI in rats with experimental liver tumours at 9.4 T. *Insights Imaging* 2013, 4:S383.
58. Kobayashi H, Brechbiel MW. Nano-sized MRI contrast agents with dendrimer cores. *Adv Drug Deliv Rev* 2005, 57:2271–2286.
59. Kobayashi H, Kawamoto S, Brechbiel MW, Bernardo M, Sato N, Waldmann TA, Tagaya Y, Choyke PL. Detection of lymph node involvement in hematologic malignancies using micromagnetic resonance lymphangiography with a gadolinium-labeled dendrimer nanoparticle. *Neoplasia* 2005, 7:984–991.
60. Koyama Y, Talanov VS, Bernardo M, Hama Y, Regino CA, Brechbiel MW, Choyke PL, Kobayashi H. A dendrimer-based nanosized contrast agent dual-labeled for magnetic resonance and optical fluorescence imaging to localize the sentinel lymph node in mice. *J Magn Reson Imaging* 2007, 25:866–871.
61. Dong Q, Hurst DR, Weinmann HJ, Chenevert TL, Londy FJ, Prince MR. Magnetic resonance angiography with gadomer-17. An animal study original investigation. *Invest Radiol* 1998, 33:699–708.
62. Misselwitz B, Schmitt-Willich H, Ebert W, Frenzel T, Weinmann HJ. Pharmacokinetics of Gadomer-17, a new dendritic magnetic resonance contrast agent. *MAGMA* 2001, 12:128–134.
63. Li D, Zheng J, Weinmann HJ. Contrast-enhanced MR imaging of coronary arteries: comparison of intra- and extravascular contrast agents in swine. *Radiology* 2001, 218:670–678.
64. Kumar K, Chang CA, Francesconi LC, Dischino DD, Malley MF, Gougoutas JZ, Tweedle MF. Synthesis, stability, and structure of gadolinium(III) and yttrium(III) macrocyclic poly(amino carboxylates). *Inorg Chem* 1994, 33:3567–3575.
65. Supkowski RM Jr, Horrocks WD. Displacement of inner-sphere water molecules from Eu<sup>3+</sup> analogues of Gd<sup>3+</sup> MRI contrast agents by carbonate and phosphate anions: dissociation constants from luminescence data in the rapid-exchange limit. *Inorg Chem* 1999, 38:5616–5619.
66. Raymond KN, Pierre VC. Next generation, high relaxivity gadolinium MRI agents. *Bioconjug Chem* 2005, 16:3–8.
67. Astashkin AV, Raitsimring AM, Caravan P. Pulsed ENDOR study of water coordination to Gd<sup>3+</sup> complexes in orientationally disordered systems. *J Phys Chem A* 2004, 108:1990–2001.
68. Caravan P, Astashkin AV, Raitsimring AM. The gadolinium(III)-water hydrogen distance in MRI contrast agents. *Inorg Chem* 2003, 42:3972–3974.
69. Fulton DA, Elemento EM, Aime S, Chaabane L, Botta M, Parker D. Glycoconjugates of gadolinium complexes for MRI applications. *Chem Commun (Camb)* 2006, 10:1064–1066.
70. Livramento JB, Helm L, Sour A, O'Neil C, Merbach AE, Toth E. A benzene-core trinuclear Gd<sup>III</sup> complex: towards the optimization of relaxivity for MRI contrast agent applications at high magnetic field. *Dalton Trans* 2008, 9:1195–1202.
71. Livramento JB, Toth E, Sour A, Borel A, Merbach AE, Ruloff R. High relaxivity confined to a small molecular space: a metallostar-based, potential MRI contrast agent. *Angew Chem Int Ed Engl* 2005, 44:1480–1484.
72. Jebasingh B, Alexander V. Synthesis and relaxivity studies of a tetranuclear gadolinium(III) complex of

- DO3A as a contrast-enhancing agent for MRI. *Inorg Chem* 2005, 44:9434–9443.
73. Ranganathan RS, Fernandez ME, Kang SI, Nunn AD, Ratsep PC, Pillai KM, Zhang X, Tweedle MF. New multimeric magnetic resonance imaging agents. *Invest Radiol* 1998, 33:779–797.
74. Holland G, Bottomley P, Hinshaw W. <sup>19</sup>F magnetic resonance imaging. *J Magn Reson* 1977, 28:133–136.
75. Ruiz-Cabello J, Barnett BP, Bottomley PA, Bulte JW. Fluorine (<sup>19</sup>F) MRS and MRI in biomedicine. *NMR Biomed* 2011, 24:114–129.
76. Fogel U, Ding Z, Hardung H, Jander S, Reichmann G, Jacoby C, Schubert R, Schrader J. In vivo monitoring of inflammation after cardiac and cerebral ischemia by fluorine magnetic resonance imaging. *Circulation* 2008, 118:140–148.
77. Stevens AN, Morris PG, Iles RA, Sheldon PW, Griffiths JR. 5-fluorouracil metabolism monitored in vivo by <sup>19</sup>F NMR. *Br J Cancer* 1984, 50:113–117.
78. Ojugo AS, McSheehy PM, McIntyre DJ, McCoy C, Stubbs M, Leach MO, Judson IR, Griffiths JR. Measurement of the extracellular pH of solid tumours in mice by magnetic resonance spectroscopy: a comparison of exogenous (<sup>19</sup>F) and (<sup>31</sup>P) probes. *NMR Biomed* 1999, 12:495–504.
79. Metcalfe JC, Hesketh TR, Smith GA. Free cytosolic Ca<sup>2+</sup> measurements with fluorine labelled indicators using <sup>19</sup>F NMR. *Cell Calcium* 1985, 6:183–195.
80. Perez-Sanchez JM, Perez de Alejo R, Rodriguez I, Cortijo M, Peces-Barba G, Ruiz-Cabello J. In vivo diffusion weighted <sup>19</sup>F MRI using SF<sub>6</sub>. *Magn Reson Med* 2005, 54:460–463.
81. Kuethe DO, Caprihan A, Gach HM, Lowe IJ, Fukushima E. Imaging obstructed ventilation with NMR using inert fluorinated gases. *J Appl Physiol (1985)* 2000, 88:2279–2286.
82. Bulte JW. Hot spot MRI emerges from the background. *Nat Biotechnol* 2005, 23:945–946.